Kinetics of Carbothermal Reduction Synthesis of Beta Silicon Carbide

Alan W. Weimer, Kevin J. Nilsen, Gene A. Cochran, and Raymond P. Roach
Ceramics and Advanced Materials Research, Dow Chemical U.S.A., Midland, MI 48667

Carbothermal reduction kinetics to synthesize SiC is studied under conditions of high carbon/silica precursor heating rates (10^5 K/s) and minimized reaction times (s) over a wide temperature range ($1{,}848 \le T \le 2{,}273$ K). The reaction mechanism includes rapid formation of a gaseous SiO intermediate. Further carbon reduction of the SiO to SiC is reaction-rate-controlling. Carbon crystallite diameter, d, has a substantial influence on the rate of reaction and the size of synthesized SiC. Fractional oxide conversion, X, can be described by a contracting volume shrinking core model:

$$k = \frac{1-(1-X)^{1/3}}{t} = \frac{k_o}{d} \exp(-E/RT)$$

where $k_o = 27.4$ m/s and $E = 382 \pm 34$ kJ/mol.

Background

Thermochemistry

Beta silicon carbide (SiC) is manufactured by the carbothermal reduction of silica (SiO_2) according to the overall reaction:

$$3\ C(s) + SiO_2(s) \Rightarrow SiC(s) + 2\ CO(g) \qquad (1)$$

Reaction 1 is highly endothermic, requiring approximately 572 kJ/mol SiC at 2,100 K.

The generally accepted reaction mechanism is that SiC is synthesized through intermediate silicon monoxide (SiO) gas. Based on this scenario, overall reaction 1 can be divided into two elementary reaction steps:

$$C(s) + SiO_2(s) \Rightarrow SiO(g) + CO(g) \qquad (2)$$

$$2\ C(s) + SiO(g) \Rightarrow SiC(s) + CO(g) \qquad (3)$$

The variation of free energy with temperature for reactions 1 to 3 at atmospheric pressure over the temperature range of interest for synthesis ($1{,}500 \le T \le 2{,}500$ K) is shown in Figure 1a. Calculations for these free energy changes have been made using the FACT (Thompson et al., 1985) database.

The overall carbothermal reduction reaction to synthesize SiC, reaction 1, has a positive standard free energy change (Figure 1a) up to about 1,793 K; so, unless carbon monoxide (CO) produced is removed from the process, a higher temperature is needed to promote reaction at a reasonable rate. The inhibiting effect of CO on kinetics at lower temperatures has been reported to be significant (Lee and Cutler, 1975; Khalafalla and Haas, 1972).

The generation of SiO via reaction 2 requires temperatures above approximately 2,025 K to proceed under equilibrium conditions at atmospheric pressure. Since reaction 3 is favorable over the entire temperature range, a reduced CO partial pressure, p_{CO}, allows overall reaction (Eq. 1) to occur at lower temperatures by improving the favorability of SiO generation via reaction 2.

The generation of SiO can result directly via solid-solid reaction (Eq. 2), SiO_2 dissociation (Klinger et al., 1966; Lee and Cutler, 1975):

$$SiO_2(s) \Rightarrow SiO(g) + 1/2\ O_2 \qquad (4)$$

$$C(s) + 1/2\ O_2(g) \Rightarrow CO(g) \qquad (5)$$

Correspondence concerning this article should be addressed to A. W. Weimer, 52 Building, Dow Chemical U.S.A., Midland, MI 48667.

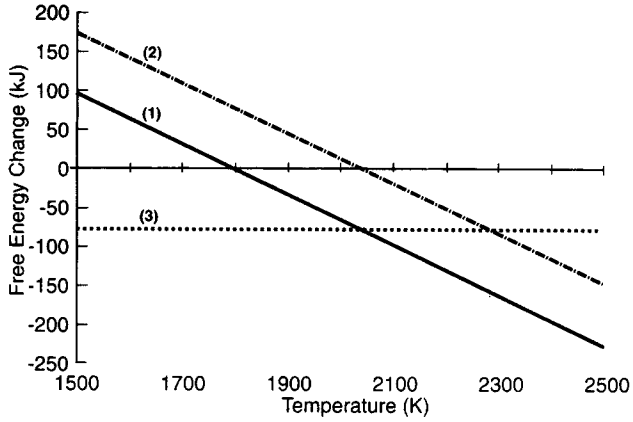

Figure 1a. Free energy change for Reactions 1, 2 and 3.

or gas-phase carbon reduction (Lee et al., 1976):

$$SiO_2(s) + CO(g) \Rightarrow SiO(g) + CO_2(g) \quad (6)$$

$$C(s) + CO_2(g) \Rightarrow 2\ CO(g) \quad (7)$$

The free energy change of SiO generation via a solid-solid mechanism (reaction 2), SiO_2 dissociation (reactions 4 and 5), and gas-phase carbon reduction (reactions 6 and 7) is shown in Figure 1b. Clearly, free energy considerations indicate that SiO is most likely generated by solid-solid reaction (Eq. 2). However, in the absence of direct carbon and silica contact, SiO could be generated by either reaction 4 or 6. Gas-phase carbon reduction via reaction 6 is favored on the basis of both free energy and enthalpy considerations.

Likewise, SiC may result from the direct carbon reduction of SiO (reaction 3), a silicon (Si) metal intermediate:

$$C(s) + SiO(g) \Rightarrow Si(s,l,g) + CO(g) \quad (8)$$

$$Si(s,l,g) + C(s) \Rightarrow SiC(s) \quad (9)$$

or gas-phase carbon reduction (Kurosawa et al., 1966; Viscomi and Himmel, 1978):

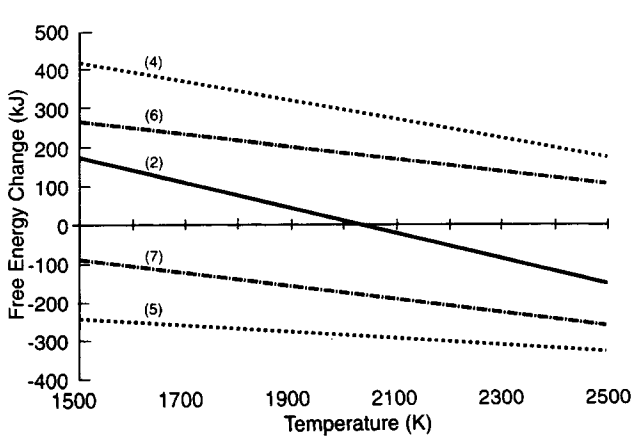

Figure 1b. Free energy change for Reactions 2 and 4-6.

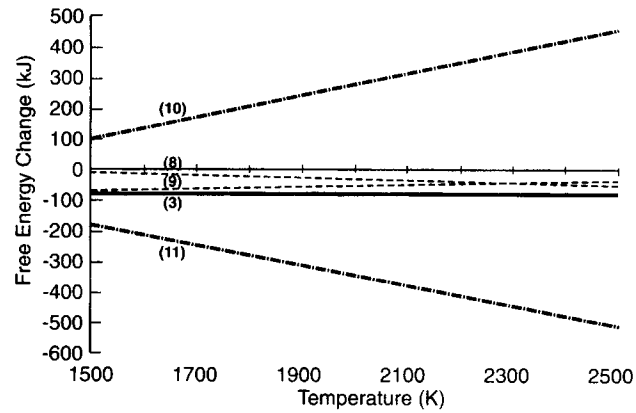

Figure 1c. Free energy change for reactions 3 and 8-11.

$$SiO(g) + 3\ CO(g) \Rightarrow SiC(s) + 2\ CO_2(g) \quad (10)$$

$$2\ C(s) + 2\ CO_2(g) \Rightarrow 4\ CO(g) \quad (11)$$

Free energy considerations regarding the synthesis of SiC from SiO are summarized in Figure 1c for reactions 3 and 8 to 11. Gas-phase SiC synthesis via CO and SiO (reaction 10) is not favorable over the entire temperature range of interest ($1{,}500 \le T \le 2{,}500$ K). It is, however, thermodynamically favorable for approximate temperatures of $T < 1{,}200$ K. This explains why several investigators (Kurosawa et al., 1966; Viscomi and Himmel, 1978) found SiC product downstream of the reaction hot zone in the cooler parts of the system. Although reactions 8 and 9 are both favorable over the entire temperature range of interest, neither is as favorable as the direct carbon reduction of SiO (reaction 3). In addition, $P_{Si(g)}$ is only about 1.1 Pa at 2,038 K (Klinger et al., 1966) indicating that Si(g) should not constitute a significant gaseous intermediate to overall reaction 1.

As indicated, overall reaction 1 may be conveniently described by consecutive reactions (Eqs. 2 and 3), each of which may proceed via more complex mechanisms as discussed.

Kinetics

A number of researchers (Blumenthal et al., 1966; Henderson and Tant, 1983; Kennedy and North, 1983; Kevorkijan et al., 1989, 1992; Khalafalla and Haas, 1972; Klinger et al., 1966; Krstic, 1992; Kurosawa et al., 1966; Kuznetsova et al., 1980; Lee et al., 1976; Lee and Cutler, 1975; Miller et al., 1979; Ono and Kurachi, 1991; Papin et al., 1972; Shimoo et al., 1990; van Dijen and Metselaar, 1991; Viscomi and Himmel, 1978; and Wei et al., 1984) have investigated the reaction kinetics of the overall carbothermal reduction reaction (Eq. 1). In general, it was found that higher temperature, finer precursor particle size, and the removal of CO increased the reaction rate.

There was some controversy as to whether or not iron catalyzed the reaction. Reported activation energies were in the range of 230 to 552 kJ/mol, depending primarily on the precursor silica and carbon sources and particle sizes.

Much controversy exists regarding the exact mechanism and controlling step in the process. Lee et al. (1976), Lee and Cutler

(1975), Kennedy and North (1983), and Krstic (1992) found reaction 1 to be controlled by the generation of SiO, reaction 2, while Viscomi and Himmel (1978) reported the reduction of SiO to SiC, reaction 3, to be rate-controlling. Several researchers (Klinger et al., 1966; Ono and Kurachi, 1991) have reported nucleation growth to be of importance, particularly for temperatures near or above the transformation temperature of quartz to cristobalite (Klinger et al., 1966). Carbon diffusion effects have been reported to be important in several studies (Ono and Kurachi, 1991; van Dijen and Metselaar, 1991). Van Dijen and Metselaar (1991) have recently rejected an SiO intermediate and suggested that overall reaction (Eq. 1) occurs through direct solid state diffusion, in which SiO_2 migrates over the SiC surface to the carbon. Wei et al. (1984) cited heat-transfer effects as being rate-controlling.

Product SiC crystal size is reportedly governed by the starting carbon crystal size, reaction temperature, and time at temperature (Kennedy and North, 1983; Kevorkijan et al., 1989, 1992; Klinger et al., 1966; and Wei et al., 1984). Klinger et al. (1966) noted that product SiC particles could not be distinguished from the starting graphite particles, while Kennedy and North (1983) and Kevorkijan et al. (1989, 1992) noted that SiC surface area decreased with higher reaction temperatures and longer reaction times, but that product SiC morphology resembled that of the starting carbon. However, Kevorkijan et al. (1989, 1992) also found that SiC crystallites synthesized at low temperature (1,443 K) corresponded to the size of the starting carbon crystallites.

In general, the reported kinetic studies for the overall carbothermal reduction reaction (Eq. 1) were carried out with larger samples in slowly heated systems (< 100 K/s) at lower temperatures (typically below 1,873 K) for extended reaction times (minutes to hours). In light of the inability to heat samples rapidly in previous studies, the reported intrinsic kinetics have been limited primarily to lower temperatures where heat-transfer resistances did not dominate. Heat-transfer resistances are of particular concern when carrying out intrinsically fast, highly endothermic reactions such as overall reaction (Eq. 1).

It is the intent of this article to better quantify the intrinsic kinetics of overall reaction (Eq. 1) and to obtain a better understanding of the reaction mechanism and the rate-limiting step. Of particular interest is whether or not overall reaction (Eq. 1) proceeds through gaseous SiO and, if it does, whether reaction 2 or 3 is rate-limiting.

Here, kinetic studies are carried out in such a manner that heat-transfer resistances are effectively eliminated. Fine "microcontainers" of reactant C/SiO_2 precursor are rapidly heated within milliseconds, held at reaction temperature for only several seconds, and immediately quenched. This is the first fundamental kinetics study for carbothermal reduction SiC synthesis to be carried out under such conditions. Intrinsic kinetics can be determined for higher reaction temperatures.

Experimental Procedure

Preparation of reactants

An intimately mixed C/SiO_2 precursor was prepared by spray drying and calcining an aqueous carbon black/silica slip. Carbon and silica sources for the precursor are summarized in Table 1. The carbon source was either a fine (C1) 72 m^2/g or slightly larger (C2) 8 m^2/g sized high-purity gas black, while the silica source was either a fine colloidal (S1) or milled 2.2 m^2/g naturally crystalline (S2) powder. As indicated in Table 1, both carbon sources were of ultra high chemical purity, while both silica sources contained similar impurity levels. By choice of these starting materials it was possible to determine the effect of reactant carbon and silica size on reaction kinetics and SiC morphology.

Table 1. Chemical and Physical Analysis of Carbon and Silica

	Carbon Source		Silica Source	
Element*	C1	C2	S1	S2
Al	< 10	< 10	760	640
Ca	< 10	< 10	< 10	290
Cl	< 10	< 10	< 10	42
Fe	12	7	123	360
Na	< 200	< 200	0.19%	< 500
S	< 10	< 10	470	25
Ti	< 10	< 10	170	79
Zr	—	—	83	< 10
C (wt. %)	98.6	98.9	—	—
O (wt. %)	0.3	0.3	—	—
d (μm)	0.030	0.218	0.022	1.1
$S.A.$ (m^2/g)	72	8	—	2.2

*ppm unless otherwise noted.

An aqueous slip of carbon black was made using alkyl phenoxy polyethoxy ethanol as a wetting agent. The silica source was added to the carbon slip for a 50 wt. % solids loading, and the combined slip was spray-dried. Colloidal silica was used as the binder for all systems. Product collected from the spray dryer was calcined at 673 K for 12 hours in a nitrogen-purged tray oven. The calcination step removed hydrated water from the silica. The spray-dried and calcined "microcontainer" C/SiO_2 precursor particles had an average volume median diameter of approximately 60 microns. Silica was insured as the limiting reactant by maintaining a molar ratio of $C/SiO_2 = 3.1$ according to overall equation (Eq. 1).

Reaction

Reaction was carried out in a rapid heating mode using a dilute transport vertical reactor process for reaction times $t < 5$ s at temperatures in the range of $1{,}848\ \text{K} \le T \le 2{,}573\ \text{K}$. The spray-dried precursor was entrained with argon gas through a cooled transport tube which extended directly into the upper reaction zone of the heated graphite flow reactor. Reaction residence time was governed by the argon flow rate, the CO generated by reaction, the tube temperature, and the volume of the reaction zone. The use of dilute flow vertical reactors for studying heterogeneous reactions has recently been discussed (Bjerle et al., 1992).

As fine cooled precursor particles were injected directly into the hot reaction zone, they were heated rapidly at the surface by radiation and gas conduction. The surface heating rate and internal particle conduction are highly dependent on particle size as well as the temperature and physical properties of the solid precursor and surrounding gas. Since the flow rate of cooled argon gas carrying the precursor particles directly into the reaction zone was small relative to the total flow rate of hot gas through the reaction zone, a reasonable assumption is

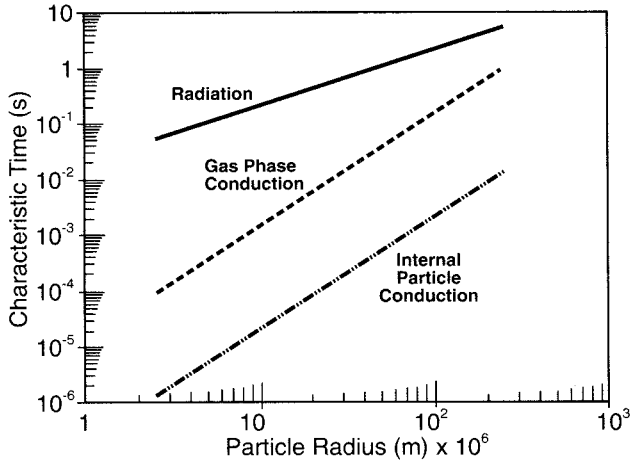

Figure 2. Precursor particle characteristic heating times.

that cooled particles instantly contact surrounding gas which is maintained at reactor wall temperature.

The characteristic heating times for spherical particles of radii between 1 and 1,000 microns are shown in Figure 2 for radiation, gas-phase conduction, and internal particle conduction for particles increasing in temperature from ambient to 2,273 K. The method of calculation has been described previously (Weimer and Clough, 1980) and is modified here to account for different physical properties. It is clear that the dominant mechanism of heating is gas-phase conduction with radiation playing a minor, but increasing, role as particles increase in size. Also, internal particle conduction is almost two orders of magnitude faster than surface heat transfer. Hence, particles are heated uniformly throughout and may be assumed to be isothermal.

Estimated particle heating rates have been calculated (Figure 3) using the dominant gas-phase conduction characteristic heating times (Figure 2). It can be seen that a characteristic heating rate of approximately 10^5 K/s is estimated for 60 micron average diameter precursor particles. This heating rate is consistent with calculations made by Celik et al. (1990) for 20 to 100 micron diameter coal particles entering an entrained flow coal devolatilization reactor.

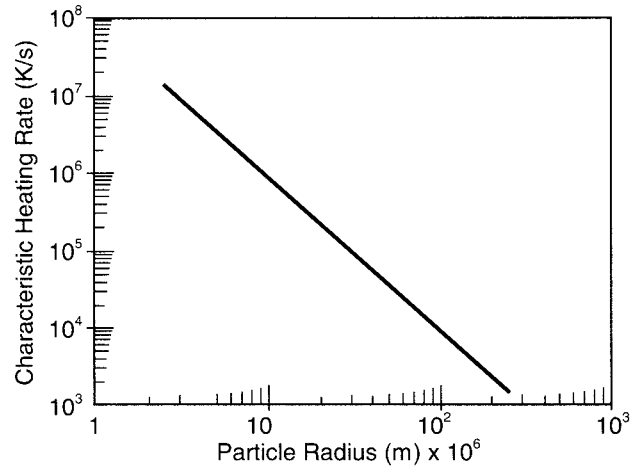

Figure 3. Precursor particle characteristic heating rate.

Analytical

Product SiC powders were analyzed chemically for carbon and oxygen using a LECO IR-412 Carbon Determinator and LECO TC-436 Oxygen Determinator, respectively. For carbon analysis using the LECO Carbon Determinator, sample material is combusted with released carbon monoxide converted to carbon dioxide in a rare earth copper oxide catalytic heater. Carbon is then measured as carbon dioxide by IR analysis. For oxygen analysis using a LECO Oxygen Determinator, the sample is pyrolyzed and released oxygen combined with carbon to form carbon monoxide. The carbon monoxide is converted to carbon dioxide as described above and the oxygen is measured by IR in the form of carbon dioxide.

Crystal-phase purity was determined by X-ray diffraction (Rigaku "Miniflex" X-ray diffractometer). Product morphology was identified by scanning electron microscopy (ISI model SS40), and surface area was determined by the BET nitrogen adsorption method using standard manufacturer's procedures (Quantochrome Corp. Autosorb-1). Trace metal impurities were quantified by X-ray fluorescence.

Silica (or oxygen) conversion in a reacted product sample was calculated as follows. Product was analyzed for total carbon and total oxygen wt. %. The remaining sample weight was assumed to be silicon. Having the total silicon and assuming that all of the oxygen was in the form of SiO_2, the amount of Si as SiC and subsequently the amount of SiC were calculated. The amount of SiO_2 reacted to yield the calculated amount of SiC could then be determined. Fractional silica (or O) conversion was then easily calculated. This method for calculating oxygen conversion was suitable because unreacted volatile oxide condensed by thermophoresis on cooled product powder exiting the reaction zone. A sample calculation is shown in the Appendix.

Results and Discussion

Product exiting the transport reactor was collected in an in-line sampling device downstream of the reactor cooling zone and analyzed as described previously.

Porous product particles (Figure 4b) maintained the spherical shape and size of the starting precursor microcontainers (Figure 4a) and contained synthesized SiC crystallites throughout. Porosity in a completely reacted precursor microcontainer particle was the result of all of the oxygen and 2/3 of the starting carbon being removed as gaseous CO according to overall reaction (Eq. 1). A realistic macroscopic scenario of the reacting microcontainer particles appears to be one in which the particles remain a constant size, but change in density as the reaction occurs uniformly throughout.

Raw product was then calcined in air to remove residual carbon, ultrasonically deagglomerated (Figure 4c), and acid treated by conventional methods (Shaffer et al., 1987) to remove residual oxygen and metal impurities.

Experiments were carried out over a wide temperature range to determine the effect of reaction parameters on crystallite size, the reaction mechanism, and the intrinsic reaction rate.

Effect of reaction parameters on SiC crystallite size

Photomicrographs (SEM) of product SiC (Figure 5) synthesized at temperatures between 2,073 and 2,573 K clearly

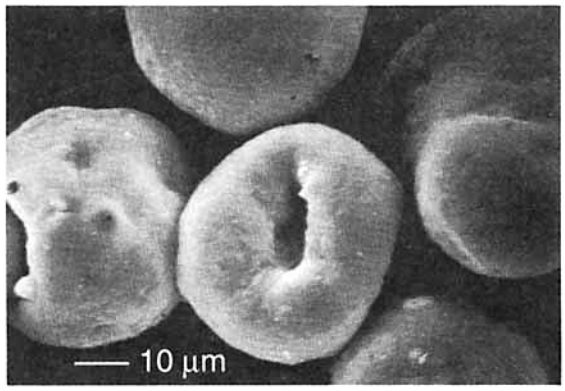

(a)

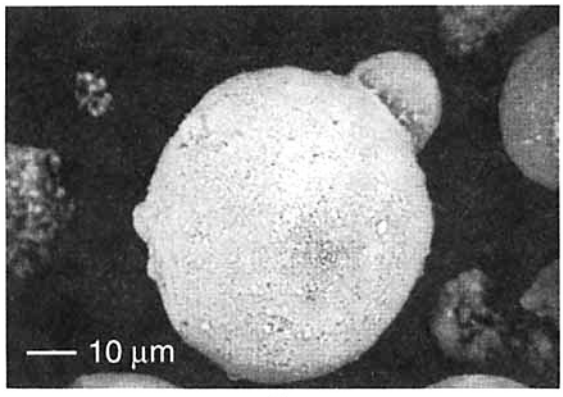

(b)

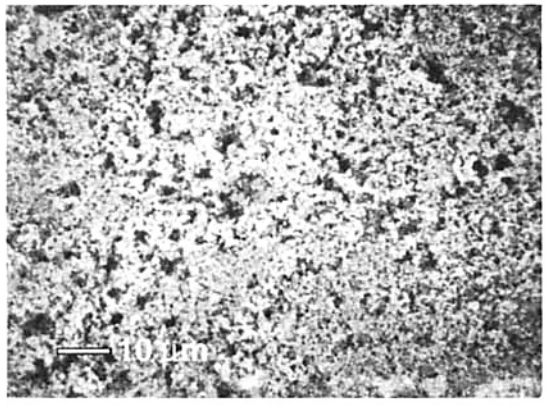

(c)

Figure 4. Spray dried precursor (C1/S1) and product SiC.

a. Precursor (C1/S1) microcontainers.
b. Product SiC particles synthesized at 2,073 K.
c. Product SiC particles after 10 min in ultrasonic bath.

indicate that SiC crystallite size increased with an increase in reaction temperature. All crystallites synthesized at temperatures below 2,573 K were less than 0.5 micron in size.

Crystallites synthesized at 2,073 K appear to be in the 0.1 to 0.2 micron size range, while those synthesized at 2,473 K appear to be in the 0.3 to 0.4 micron size range. The 2,573 K product is sintered (Figure 5d), indicative of reaction temperature exceeding the sintering temperature of SiC.

Crystallite size was quantified through extensive TEM char-

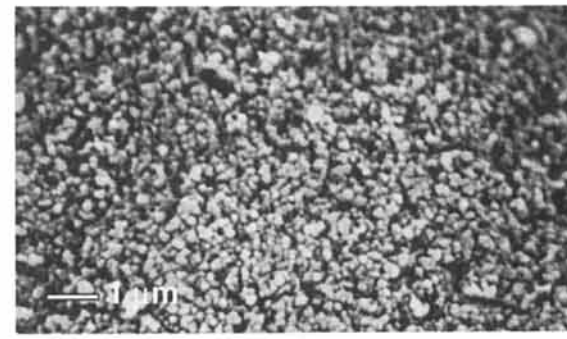

(a)

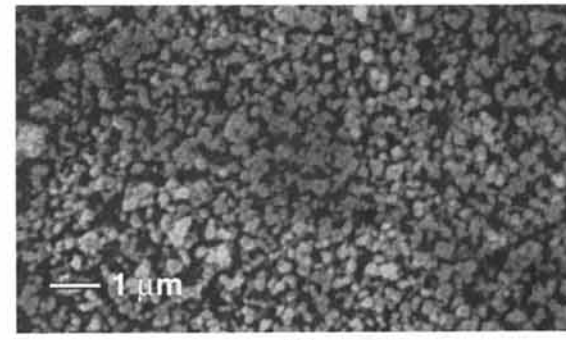

(b)

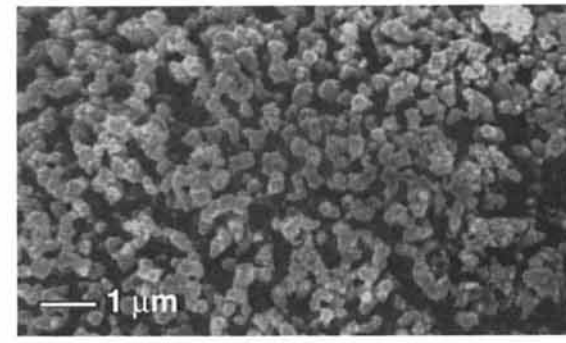

(c)

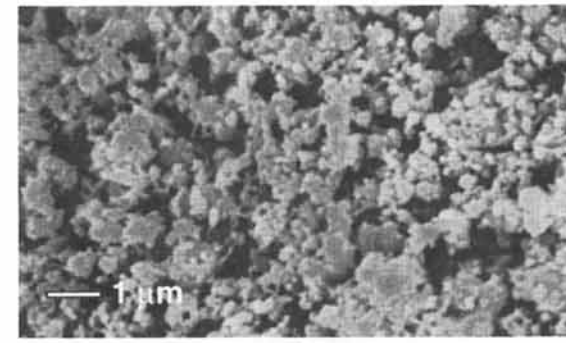

(d)

Figure 5. Product SiC particles synthesized from (C1/S1) precursor.

a. 2,073 K; b. 2,173 K; c. 2,473 K; d. 2,573 K.

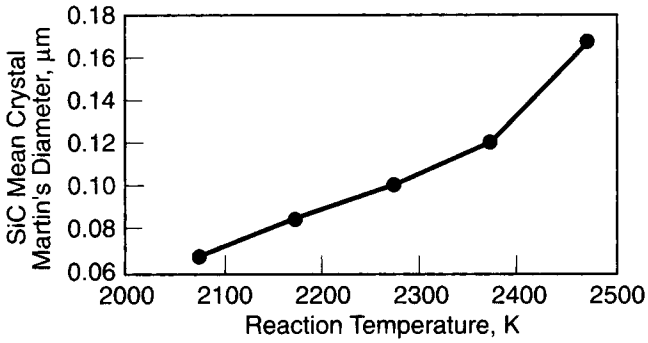

Figure 6. Effect of temperature on mean SiC crystallite size synthesized from (C1/S1) precursor.

acterization and subsequent crystal size distribution analysis. Martin's diameters (Martin et al., 1924) were measured from randomly obtained TEM's and statistically analyzed to quantify the mode, median, mean and standard deviation. The mean crystallite size varies with temperature as shown in Figure 6. The crystallite-size distributions for these powders are very narrow as shown in Figure 7 for the 2,173 K synthesized product which has a coefficient of variation of $s_v = 0.34$.

Starting carbon crystallite size also has a substantial influence on the resulting SiC crystallite size as shown by the photomicrographs of Figure 8. Here, the product SiC synthesized at $T = 2{,}323$ K (Figure 8b) from the C2/S2 precursor (Figure 8a) comprises crystallites which resemble the starting C2 carbon (Figure 8a).

Also, a comparison of the photomicrographs of the C2 carbon derived SiC product at $T = 2{,}323$ K (Figure 8b) with the C1 carbon derived SiC product at $T = 2{,}173$ K (Figure 5b) and $T = 2{,}473$ K (Figure 5c) further substantiates the conclusion that SiC crystallite size resembles the starting carbon size. Here, the C1 carbon derived SiC (Figures 5a,b,c) is finer than the C2 derived SiC (Figure 8b) at comparable temperatures. These results are consistent with reported observations of Kennedy and North (1983), Kevorkijan et al. (1989, 1992), Klinger et al. (1966), and Wei et al. (1984).

Starting silica size appears to have no influence, as the submicron-sized SiC crystallites (Figure 8b) show no resemblance to the angular 1.1 micron mean sized S2 silica reactant (Figure 8a and Table 1).

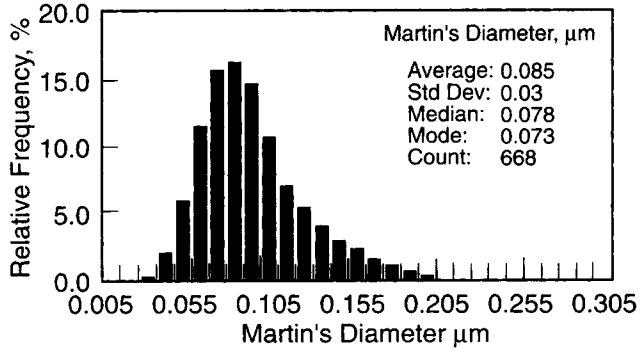

Figure 7. Martin's diameter SiC crystallite size distribution.

$T = 2{,}173$ K; C1/S1 precursor.

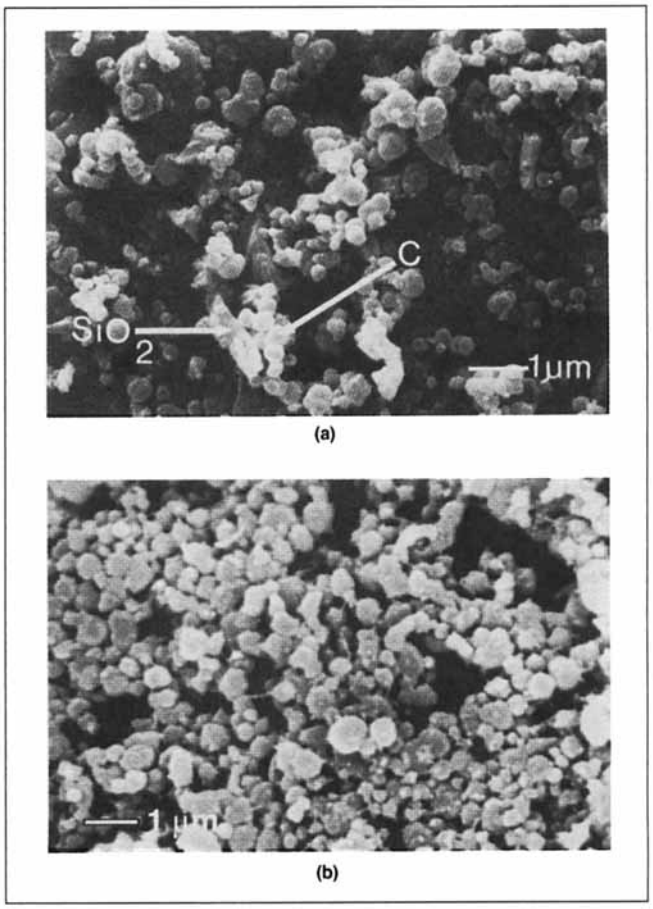

Figure 8. (C2/S2) precursor and product SiC.

a. (C2/S2) precursor.
b. SiC Product ($T = 2{,}323$ K).

A realistic physical scenario of chemical reaction within the microcontainer particles is one in which the initial SiC crystallites resemble the starting carbon crystallites and then, once formed, grow by a sintering process to larger crystallites. Finer carbon crystallites such as C1 are more reactive (to be discussed) and may allow grain growth to occur at lower temperatures (since SiC has been synthesized) relative to larger carbon crystallites such as C2. It appears that SiC grain growth does not substantially occur as long as carbon is available for reaction to SiC. This indicates that either the carbothermal reduction reaction kinetics to SiC is much faster than SiC grain growth or that free carbon inhibits SiC grain growth.

Reaction mechanism

Photomicrographs (Figure 9) and X-ray diffraction studies (Figure 10) of partially reacted particles exiting the reactor cooling zone suggest that reaction occurs throughout the precursor microcontainer particles and that, at low silica (or oxygen) conversion, volatile, unreacted oxides condense as a fibrous species on the exiting microcontainer particles. The condensation most likely occurs as a thermophoresis phenomenon during rapid cooling of the incompletely reacted particles upon entering the cooling zone. The extent of this condensation is shown in Figure 9 at various magnifications for partially

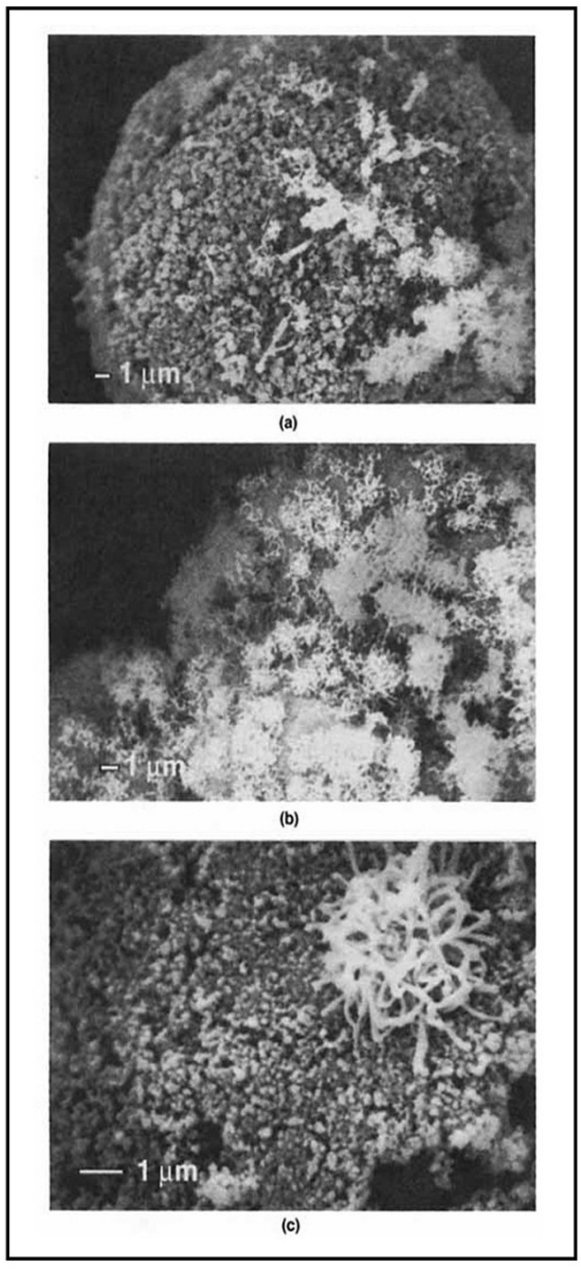

Figure 9. Partially reacted raw product SiC powders from (C1/S1) precursor.

$T = 1{,}898$ K; $X = 0.22$.
a. 2,500× magnification; b. 3,000× magnification; c. 10,000× magnification.

converted ($X = 0.22$) microcontainer particles reacted at 1,898 K for approximately 4 s.

X-ray diffraction patterns (Figures 10a,b) for low conversion/temperature products indicate the presence of crystalline silicon (Si) metal. Free Si metal was not detected in the X-ray diffraction patterns of highly converted products and is associated with the fibrous condensed species as determined by X-ray microprobes.

It is believed that the Si was most likely formed by disproportionation of gaseous SiO on cooling according to the reaction:

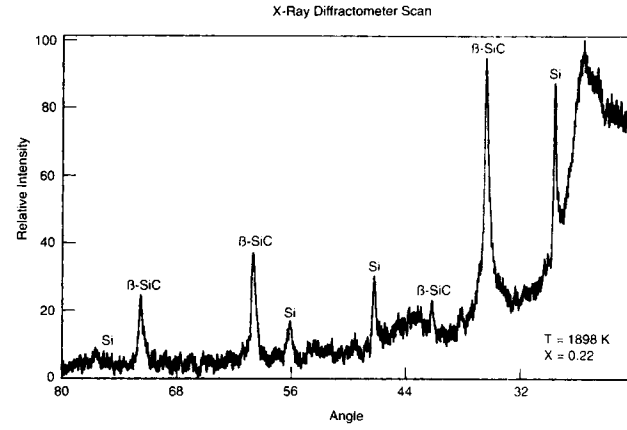

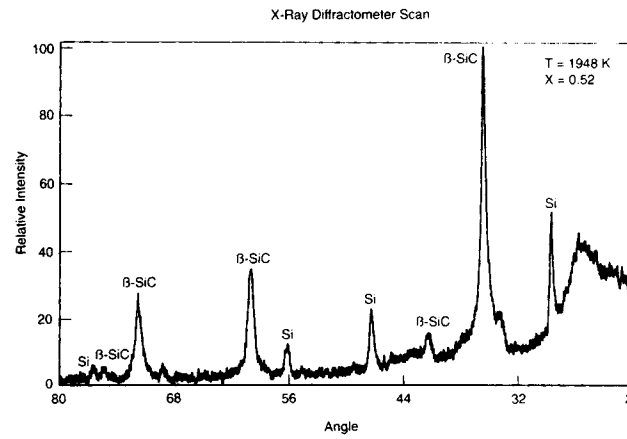

Figure 10. X-ray diffraction pattern for partially converted raw SiC powders (from C1/S1 precursor).

a. $T = 1{,}898$ K; $X = 0.22$.
b. $T = 1{,}948$ K; $X = 0.52$.

$$2\ \mathrm{SiO(g)} \Rightarrow \mathrm{SiO_2(s)} + \mathrm{Si(s,l)} \qquad (12)$$

Free energy change considerations for reaction 12 indicate that Si(s,l) formation is favorable at temperatures below approximately 2,132 K.

These results provide substantial evidence that overall reaction (Eq. 1) occurs via a gaseous SiO intermediate and that the formation of SiO(g) is fast. Initially, SiO(g) is most likely formed rapidly according to reaction 2 when carbon and silica particles are in contact. The high rate of SiO(g) synthesis suggests that the CO produced by reaction 2 reacts with SiO_2 to synthesize SiO(g) according to reaction 6. The CO_2 which is formed then reacts with carbon (reaction 7) to synthesize CO, which, in turn, reacts with silica according to reaction 6 to continue the cycle. Reaction 2 is feasible only at points of direct contact between C and SiO_2, and hence takes place during the initial period only. After the direct contact points are consumed, reaction 2 most likely ceases. Hence, reactions 6 and 7 are the ones which make reaction 3 possible.

Experiments were carried out to determine the effect of

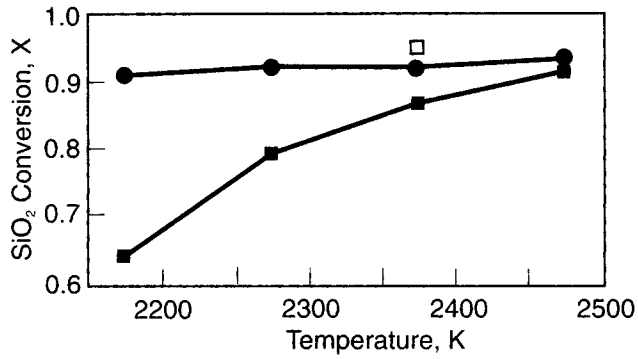

Figure 11. Effect of carbon and silica crystallite size on reaction kinetics.

Equivalent gas/solid feed rates & precursor composition.
• (C1/S1) precursor; □ (C1/S2) precursor; ■ (C2/S2) precursor.

carbon and silica crystallite size on the rate of reaction. Microcontainer precursors of identical molar $C/SiO_2 = 3.1$ composition were prepared using C1/S1, C1/S2, and C2/S2 reactants. These precursors were reacted under identical single pass rapid heating conditions (identical gas/solid feed rates at various temperatures) in order to quantify the effect of starting carbon and silica crystallite size on reaction rate. The effect of crystallite size on conversion at various temperatures (2,173 K $\leq T \leq$ 2,473 K) is shown in Figure 11.

It appears, from a comparison of the C1/S1 and C1/S2 results at $T = 2{,}373$ K (Figure 11), that starting silica crystallite size has no effect on the rate of reaction. Here, an increase in silica crystallite size of approximately 37 times results in single-pass product of nearly equivalent, but unexpectedly higher, oxide conversion.

Starting carbon crystallite size, however, appears to have a significant influence on the reaction rate. A comparison of powders synthesized from the C1/S1 and C2/S2 precursors over the entire temperature range clearly indicates that larger-sized carbon crystallites are substantially less reactive. At $T = 2{,}173$ K, the C2 containing precursor only achieves a silica conversion of $X = 0.63$, while the C1 containing precursor achieves a much higher $X = 0.91$ conversion level. This difference is reactivity holds over the entire temperature range, although the degree of difference decreases with increasing temperature. High silica conversions can be achieved for the larger sized carbon crystallite containing precursors at higher temperatures (that is, $X > 0.90$ for $T > 2{,}473$ K).

In summary, rapid reaction rates which complete overall reaction (Eq. 1) in seconds, substantial quantities of unreacted SiO(g) exiting the reactor under more mild conditions, the increase in reaction rate with finer carbon crystallite size, the independence of rate on silica size, and the fact that SiC crystallites resemble the starting carbon crystallites suggest that overall reaction (Eq. 1) most likely occurs through an SiO(g) intermediate via reactions 2, 6, 7 and 3, and that reaction 3 is rate-limiting.

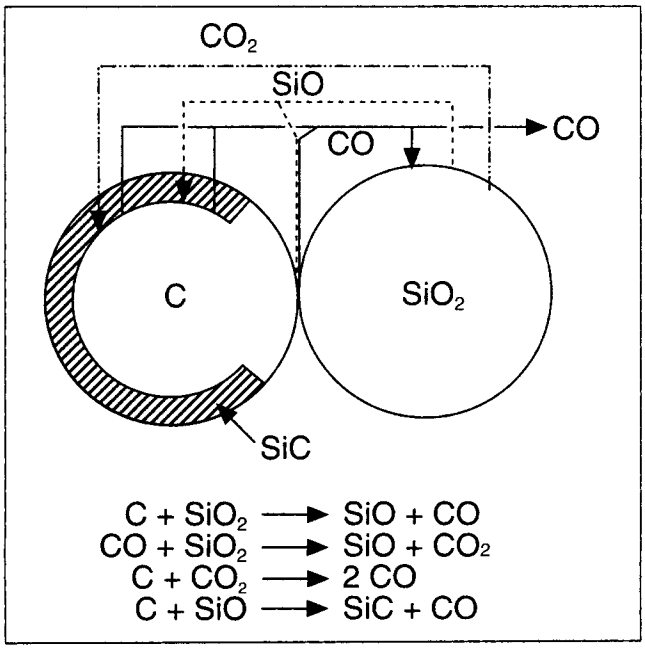

Figure 12. Proposed reaction mechanism.

Intrinsic reaction rate

To quantify the intrinsic reaction rate, kinetic experiments achieving a wide silica conversion level ($0.14 \leq X \leq 0.83$) were carried out over a wide temperature range (1,848 K $\leq T \leq$ 2,273 K) for various short residence times ($2.5 \leq t \leq 4.3$ s).

In view of the fact that SiC crystal size and morphology initially (prior to grain growth) reflect that of the starting carbon and the fact that SiO(g) is an intermediate in the reaction as discussed previously, a suitable and simple gas/solid kinetic model appears to be one in which reaction proceeds at the surface of the carbon according to a shrinking core model (Yagi and Kunii, 1955). As the SiC product layer grows, the reaction surface decreases and leads to a decrease in the rate of reaction. A schematic of this mechanistic model for SiC synthesis according to reactions 2, 3, 6 and 7 is shown in Figure 12.

For an irreversible phase boundary controlled reaction of spherical carbon particles for which the thickness of the reaction zone is small compared with the dimensions of the particle:

$$k = \frac{1-(1-X)^{1/3}}{t} = \frac{k_o}{d}\exp(-E/RT) \qquad (13)$$

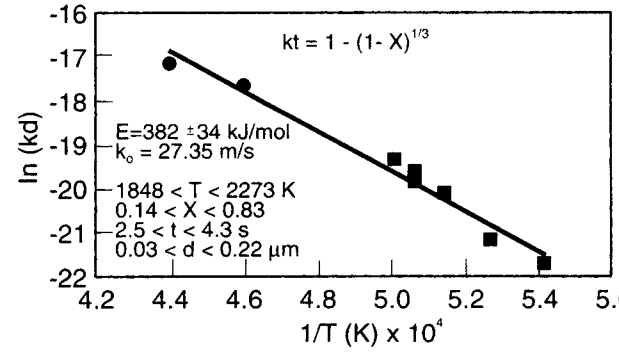

Figure 13. Reaction kinetics for contracting volume model with phase boundary control—Eq. 13.

■ C1 carbon; • C2 carbon.

where

$$k_o = \frac{4k_{so}C_{SiO}}{\rho_c} \tag{14}$$

for reaction 3 being rate-controlling. Since the surface concentration, C_{SiO}, is unknown, the preexponential factor, k_{so}, cannot be determined. However, the activation energy, E, and rate parameter, k_o, can be determined as shown in Figure 13 where the low temperature/conversion kinetic results obtained for the C1 and C2 containing precursors are linearly fit to Eq. 13.

Comparison to reported results

The reaction rates, k, and activation energy, E (382 ± 34 kJ/mol), reported in this work are generally consistent with previously reported results as shown in Table 2. The broad range of activation energies reported ($251 \le E \le 552$ kJ/mol) is most likely due to the broad range of rate equation forms which have been fit to the data. The differences in reaction rates are consistent with differences in carbon source reactivity and crystallite size. For example, the lower rates reported by Klinger et al. (1966) are expected for the reaction of large, low reactivity, graphite particles. In addition, petroleum coke generally contains metal impurities which are known to increase reaction

Table 2. Comparative Reaction Rate and Activation Energy

Reference	Carbon				
	Source	d (μm)	T (K)	k (s^{-1})	E (kJ/mol)
Blumenthal et al. (1966)	carbon black	0.017	1,573	1.0×10^{-3}	287
			1,673	5.7×10^{-3}	
			1,773	1.5×10^{-2}	
Khalafalla and Haas (1972)	graphite	—	1,673	1.4×10^{-3}	322
			1,698	1.7×10^{-3}	
			1,723	1.9×10^{-3}	
			1,788	2.8×10^{-3}	
Klinger et al. (1966)	graphite	<44	1,818	3.2×10^{-7}	510
			1,863	4.5×10^{-7}	
			1,913	1.7×10^{-6}	
			1,943	2.3×10^{-6}	
			1,983	4.5×10^{-6}	
			2,038	1.4×10^{-5}	
Kuznetsova et al. (1980)	carbon black	0.187	1,773	1.7×10^{-2}	251
			1,873	5.8×10^{-2}	
			1,973	7.6×10^{-2}	
			2,073	2.1×10^{-1}	
	carbon black	0.385	1,773	7.8×10^{-3}	288
			1,873	2.8×10^{-2}	
			1,973	6.2×10^{-2}	
			2,073	1.3×10^{-1}	
	coke	0.198	1,773	9.2×10^{-3}	299
			1,873	3.1×10^{-2}	
			1,973	6.2×10^{-2}	
			2,073	1.6×10^{-1}	
Lee and Cutler (1975)	charcoal	70	1,623	5.0×10^{-4}	544
			1,643	1.0×10^{-3}	
			1,673	1.5×10^{-3}	
			1,703	3.9×10^{-3}	
			1,713	4.0×10^{-3}	
Ono and Kurachi (1991)	pyrolyzed polymer	—	1,795	3.2×10^{-3}	391
			1,813	3.5×10^{-3}	
			1,821	5.5×10^{-3}	
			1,881	1.2×10^{-2}	
			1,962	2.7×10^{-2}	
Shimoo et al. (1990)	pyrolyzed polymer	—	1,773	1.5×10^{-2}	352
			1,873	2.7×10^{-2}	
			1,973	4.5×10^{-2}	
Viscomi and Himmel (1978)	coke breeze	—	1,673	1.1×10^{-2}	552
			1,723	1.4×10^{-2}	
			1,773	2.5×10^{-2}	
This work	carbon black	0.030	1,848	1.2×10^{-2}	382
			1,898	2.0×10^{-2}	
			1,948	6.2×10^{-2}	
			1,973	8.9×10^{-2}	
			1,998	1.3×10^{-1}	
		0.218	2,173	9.2×10^{-2}	
			2,273	1.5×10^{-1}	

rates as shown by the data of Kuznetsova et al. (1980) and Viscomi and Himmel (1978). Carbon from pyrolyzed polymers is generally very reactive as indicated by the rates reported by Ono and Kurachi (1991) and Shimoo et al. (1990).

The reaction rates estimated for previously reported carbon blacks (Blumenthal et al., 1966; Kuznetsova et al., 1980), using the rate equation derived in this work, are slightly lower than those reported by the previous investigators. This may be the result of differences in metal impurities within the carbon blacks. The carbon sources used in this work are of ultra high purity (Table 1). The purity of carbon in the previous studies was not reported.

The rates reported in this work include higher temperature (up to $T = 2{,}273$ K) reaction rates which have never been reported previously. The rapid heating of small samples allowed heat-transfer resistances to be effectively eliminated and intrinsic kinetics to be determined at the higher temperatures. In addition, the effect of carbon crystallite diameter, d, is, for the first time, explicitly contained in the reaction rate expression.

Conclusions

Overall reaction (Eq. 1) is intrinsically fast and may be completed in several seconds at temperatures in excess of approximately 2,100 K. The reaction appears to proceed through a rapidly formed SiO(g) intermediate synthesized according to reactions 2, 6 and 7. Solid/solid reaction (Eq. 2) most likely occurs at the contact points of the carbon and silica. However, the rapid reaction rates indicate that the gas/solid mechanism through reactions 6 and 7 is most important.

The presence of substantial unreacted SiO(g) exiting the reactor indicates that the generation of SiO(g) is fast and that the overall reaction is controlled by the reduction of SiO(g) to synthesize SiC (reaction 3). Further evidence for reaction 3 being rate controlling is provided by the fact that carbon crystallite size has a substantial effect on the rate of reaction while the size of the starting silica is of no influence.

Initially synthesized SiC crystallites resemble the starting carbon crystallites in size and morphology and, once formed, grow by a sintering process to larger crystallites. Substantial SiC grain growth does not appear to occur as long as sufficient carbon is available for reaction to SiC.

The macroscopic reaction of spray dried precursor microcontainers of starting carbon and silica may be described as spheres of constant size which change in density as reaction occurs uniformly throughout. Internally, a realistic kinetic model appears to be one in which reaction proceeds at the surface of the carbon. The reaction rate decreases as the growing SiC product layer decreases the reaction surface area and may be described by a shrinking core model:

$$k = \frac{1-(1-X)^{1/3}}{t} = \frac{27.4}{d}\exp(-382{,}000/\mathrm{RT}) \qquad (15)$$

The intrinsically fast reaction kinetics of highly endothermic overall reaction (Eq. 1) will force slow heating rate SiC production processes to be throughput-limited by heat transfer.

Acknowledgment

The authors would like to thank Dow Chemical employees David Susnitzky, Charles Wood, Harold Klassen and Don Beaman for their analytical support.

Notation

C_{SiO} = concentration of SiO, mol/m^3
d = carbon crystallite diameter, m
E = activation energy, kJ/mol
k = reaction rate, Eq. 13, s^{-1}
k_o = rate parameter, Eq. 13, m/s
k_{so} = preexponential factor, m/s
s_v = coefficient of variation
t = time, s
T = temperature, K
R = gas law constant, 8.314 J/mol·K
X = silica (or oxygen) conversion
ρ_c = carbon molar density, mol/m^3

Literature Cited

Bjerle, I., F. Xu, and Z. Ye, "Useful Experimental Technique for the Study of Heterogeneous Reactions," *Chem. Eng. Technol.*, **15**, 151 (1992).

Blumenthal, J. L., M. J. Santy, and E. A. Burns, "Kinetic Studies of High-Temperature Carbon-Silica Reactions in Charred Silica-Reinforced Phenolic Resins," *AIAA J.*, **4**(6), 1053 (1966).

Celik, I., T. J. O'Brien, and D. B. Godbole, "A Numerical Study of Coal Devolatilization in an Entrained-Flow Reactor," *Chem. Eng. Sci.*, **45**, 65 (1990).

Henderson, J. B., and M. R. Tant, "A Study of the Kinetics of High-Temperature Carbon-Silica Reactions in an Ablative Polymer Composite," *Poly. Composites*, **4**(4), 233 (1983).

Kennedy, P., and B. North, "The Production of Fine Silicon Carbide Powder," *Fabrication Science 3*, D. Taylor, ed., British Ceram. Soc., Shelton, No. 33, 1 (1983).

Kevorkijan, V., M. Komac, and D. Kolar, "The Influence of Preparation Conditions on the Properties of Beta SiC Powders Synthesized by Carbothermic Reduction," *Ceram. Powd. Proc. Sci. Proc. Int. Conf.*, 327 (1989).

Kevorkijan, V., M. Komac, and D. Kolar, "Low-Temperature Synthesis of Sinterable SiC Powders by Carbothermal Reduction of Colloidal SiO_2," *J. Mat. Sci.*, **27**(10), 2705 (1992).

Khalafalla, S. E., and L. A. Haas, "Kinetics of Carbothermal Reduction of Quartz Under Vacuum," *J. Amer. Ceram. Soc.*, **55**, 414 (1972).

Klinger, N., E. L. Strauss, and K. L. Komarek, "Reactions Between Silica and Graphite," *J. Amer. Ceram. Soc.*, **49**, 369 (1966).

Krstic, V. D., "Production of Fine, High-Purity Beta Silicon Carbide Powders," *J. Amer. Ceram. Soc.*, **75**(1), 170 (1992).

Kurosawa, T., T. Kikuchi, and T. Yagihashi, "Carbothermic Reduction of Silica," *Proc. Meml. Lect. Meet. Anniv. Found. Natl. Res. Inst. Met.*, National Research Institute of Metals, Nakameguro, Japan, 114 (1966).

Kuznetsova, V. L., V. A. Dmitrenko, and A. D. Kokurin, "Kinetics of Formation of Silicon Carbide," *Proc. of the Mendeleev Chem. Soc., Zh. Vses. Khim. O-VA*, **25**(1), 118 (1980).

Lee, J.-G., P. D. Miller, and I. B. Cutler, "Carbothermal Reduction of Silica," *Reactivity of Solids*, J. Wood, O. Lindqvist, C. Helgesson, and N.-G. Vannerberg, eds., Plenum, 707 (1976).

Lee, J.-G., and I. B. Cutler, "Formation of Silicon Carbide from Rice Hulls," *Ceramic Bulletin*, **54**, 195 (1975).

Martin, G., C. E. Blyth, and H. Tongue, "Researches on the Theory of Fine Grinding: VII," *Trans. Ceram. Soc. (Eng.)*, **23**, 61 (1924).

Miller, P. D., J.-G. Lee, and I. B. Cutler, "The Reduction of Silica with Carbon and Silicon Carbide," *J. Amer. Ceram. Soc.*, **62**, 147 (1979).

Ono, K., and Y. Kurachi, "Kinetic Studies on Beta SiC Formation from Homogeneous Precursors," *J. Mat. Sci.*, **26**, 388 (1991).

Papin, G. G., I. V. Ryabchikov, V. G. Mizin, G. V. Serov, and N. M. Dekhanov, "Reaction of Quartz with Carbon Reducing Agents," *Khimiya Tverdogo Topliva*, No. 1, 101 (1972).

Shaffer, P. T. B., K. A. Blakely, and M. A. Janney, "Production of Fine, High-Purity, Beta SiC Powder," *Ceramic Powder Science*, G. L. Messing, K. S. Mazdiyasni, J. W. McCauley, and R. A. Haber, eds., Amer. Ceram. Soc., 257 (1987).

Shimoo, T., M. Sugimoto, and K. Okamura, "Synthesis of Silicon Carbide Powders from Organosilicon Polymers," *Funtai Oyobi Funmatso Yakin*, **37**(11), 1132 (1990).
Thompson, W. T., A. D. Pelton, and C. W. Bale, *Facility for the Analysis of Chemical Thermodynamics [FACT]*, Thermfact Ltd., Mount-Royal, Quebec, Canada (1985).
Van Dijen, F. K., and R. Metselaar, "Chemical Reaction Engineering Aspects of a Rotary Reactor for Carbothermal Synthesis of SiC," *J. Eur. Ceram. Soc.*, **5**, 55 (1989).
Van Dijen, F. K., and R. Metselaar, "The Chemistry of the Carbothermal Synthesis of Beta SiC: Reaction Mechanism, Reaction Rate and Grain Growth," *J. Europ. Ceram. Soc.*, **7**, 177 (1991).
Viscomi, F., and L. Himmel, "Kinetic and Mechanistic Study on the Formation of Silicon Carbide from Silica Flour and Coke Breeze," *J. Metals*, No. 6, 21 (1978).
Wei, G. C., C. R. Kennedy, and L. A. Harris, "Synthesis of Sinterable SiC Powders by Carbothermic Reduction of Gel-Derived Precursors and Pyrolysis of Polycarbosilane," *Ceram. Bulletin*, **63**, 1054 (1984).
Weimer, A. W., and D. E. Clough, "Modeling of Char Particle Size/Conversion Distributions in a Fluidized Bed Gasifier: Non-Isothermal Effects," *Powd. Technol.*, **27**, 85 (1980).
Yagi, S., and D. Kunii, *Proc. Int. Symp. Combustion*, Van Nostrand Reinhold, New York, 231 (1955).

Appendix: Example Calculation of Silica (or Oxygen) Conversion

Assumptions. Product composition is SiC, SiO_2, and free *C* only. All unreacted volatile oxides deposit by thermophoresis on the raw product on entering the cooling zone (see Figure 9) and are accounted for as SiO_2. The amount of free Si metal is negligible (crystalline Si metal strongly diffracts and even minute quantities [<0.5%] have relatively large X-ray diffraction peak intensities, Figure 10).

Analytical composition of raw product: 44.06 wt. % total C
19.83 wt. % total O

$$\text{wt. \% total Si} = 100 - \text{wt. \% C} - \text{wt. \% O}$$
$$= 36.11$$

$$\text{wt. \% } SiO_2 = (60.09/32) \times (\text{wt. \% O})$$
$$= 37.24$$

$$\text{wt. \% Si as } SiO_2 = (28.09/60.09) \times (\text{wt. \% } SiO_2)$$
$$= 17.41$$

$$\text{wt. \% Si as SiC} = \text{wt. \% total Si} - (\text{wt. \% Si as } SiO_2)$$
$$= 18.7$$

$$\text{wt. \% SiC} = (40.1/28.09) \times (\text{wt. \% Si as SiC})$$
$$= 26.7$$

$$\text{wt. \% } SiO_2 \text{ required to yield SiC} = (60.09/40.1) \times (\text{wt. \% SiC})$$
$$= 40.01$$

$$\text{wt. \% Initial } SiO_2 = (\text{wt. \% } SiO_2) + (\text{wt. \% } SiO_2 \text{ required to yield SiC})$$
$$= 77.25$$

$$\text{\% } SiO_2 \text{ Conversion} = 100 \times (\text{wt. \% Initial } SiO_2 - \text{wt. \% } SiO_2)/(\text{wt. \% Initial } SiO_2)$$
$$= 51.79$$

Manuscript received Mar. 27, 1992, and revision received Sept. 2, 1992.